Published in final edited form as:
Nat Struct Mol Biol. 2009 December ; 16(12): 1218–1223. doi:10.1038/nsmb.1702.

Structural basis of ligand binding by a c-di-GMP riboswitch

Kathryn D Smith[1], **Sarah V Lipchock**[1], **Tyler D Ames**[2], **Jimin Wang**[3], **Ronald R Breaker**[2,3,4], and **Scott A Strobel**[1,3]

[1]Department of Chemistry, Yale University, New Haven, Connecticut, USA

[2]Department of Molecular, Cellular and Developmental Biology, Yale University, New Haven, Connecticut, USA

[3]Department of Molecular Biophysics and Biochemistry, Yale University, New Haven, Connecticut, USA

[4]Howard Hughes Medical Institute, Yale University, New Haven, Connecticut, USA

Abstract

The second messenger signaling molecule bis-(3′-5′)-cyclic dimeric guanosine monophosphate (c-di-GMP) regulates many processes in bacteria, including motility, pathogenesis, and biofilm formation. c-di-GMP–binding riboswitches are important downstream targets in this signaling pathway. Here we report the crystal structure, at 2.7 Å resolution, of a c-di-GMP riboswitch aptamer from *Vibrio cholerae* bound to c-di-GMP, showing that the ligand binds within a three-helix junction that involves base-pairing and extensive base-stacking. The symmetric c-di-GMP is recognized asymmetrically with respect to both the bases and the backbone. A mutant aptamer was engineered that preferentially binds the candidate signaling molecule c-di-AMP over c-di-GMP. Kinetic and structural data suggest that genetic regulation by the c-di-GMP riboswitch is kinetically controlled and that gene expression is modulated through the stabilization of a previously unidentified P1 helix, illustrating a direct mechanism for c-di-GMP signaling.

c-di-GMP is a second messenger signaling molecule that regulates many vital processes within the bacterial kingdom. c-di-GMP concentrations regulate the transition from a motile, planktonic lifestyle to a sessile, biofilm-forming state[1]. In general, when levels of c-di-GMP rise in the cell, biofilm formation is induced, often by upregulation of the cellular machinery necessary to create the exopolysaccharide material necessary for the development of a biofilm. Inversely, many species selectively degrade c-di-GMP under conditions conducive to a motile lifestyle, initiating the transition to a planktonic state[1,2]. This signaling pathway also plays an important role in controlling the virulence response in many organisms, with increases in c-di-GMP leading to inhibition of virulence genes. Levels of c-di-GMP are often decreased during infection, allowing the bacterium to express virulence factors necessary to survive in the host[3]. c-di-GMP is also involved in broader signaling processes,

Correspondence should be addressed to S.A.S. (scott.strobel@yale.edu)..

AUTHOR CONTRIBUTIONS

K.D.S. determined the crystal structure, performed biochemical experiments, and wrote the manuscript. S.V.L. performed biochemical experiments. T.D.A. performed the updated sequence alignment and performed the in-line probing experiments. J.W. gave critical help in data processing and refinement. R.R.B. and S.A.S. advised on the project. All authors discussed the data and provided comments on the manuscript.

Accession codes. Protein Data Bank: The atomic coordinates and structure factors for the c-di-GMP bound riboswitch have been deposited with accession code 3IRW.

COMPETING INTERESTS STATEMENT

The authors declare competing financial interests: details accompany the full-text HTML version of the paper at http://www.nature.com/nsmb/.

as it interacts with both the quorum sensing[4] and cAMP[5] signaling pathways, underscoring the importance and widespread effects of this second messenger.

Despite many advances in understanding the effects of c-di-GMP signaling, the molecular view of how this molecule interacts with downstream targets to create phenotypic changes is still incomplete[1,3,6,7]. A class of riboswitches, called GEMM, was recently identified that binds c-di-GMP with high affinity and regulates gene expression in response to c-di-GMP binding[8]. Riboswitches are RNA elements that reside in the 5′ untranslated region (UTR) of genes and modulate their expression using either transcriptional or translational mechanisms. These RNAs contain two domains: one that recognizes the ligand, called the aptamer, and one that controls gene expression in response to binding, called the expression platform[9]. More than 500 examples of the c-di-GMP riboswitch have been found within the 5′ UTR of genes in many bacteria, including the causative agents of anthrax and cholera8. Consistent with the observed role of c-di-GMP in biological function, genes regulated by c-di-GMP riboswitches include those involved in pilus assembly, motility, chemotaxis sensing and pathogenesis8. Because the c-di-GMP riboswitch class binds c-di-GMP and regulates the expression of a broad spectrum of genes in response to binding to this second messenger, it is expected to be a primary downstream target in this signaling pathway and is the first example of an RNA involved in intracellular signaling8.

Based on genomic sequence and biochemical analysis, the c-di-GMP aptamer RNA was predicted to form a conserved secondary structure with at least two stems, P1 and P2 (renamed in Fig. 1 as P2 and P3). Additionally, nucleotides flanking the two helices are necessary for c-di-GMP binding, but only the bases closest to the stems are conserved. These flanking residues become more structured upon c-di-GMP binding as seen by modulations in the in-line probing pattern[8].

To understand the structural basis of RNA-mediated c-di-GMP signaling, we have solved the crystal structure of a c-di-GMP riboswitch from *V. cholerae* bound to c-di-GMP. The structure reveals the details of second messenger binding to the RNA and suggests a mechanism by which c-di-GMP binding may trigger this molecular switch.

RESULTS

Structure determination of the c-di-GMP riboswitch

We have determined the 2.7 Å resolution crystal structure of the c-di-GMP riboswitch aptamer (Vc2) upstream of the *tfoX*-like gene in *V. cholerae* bound to c-di-GMP (Fig. 1). This gene has been shown to be upregulated in *V. cholerae* mutants with the rugose phenotype, characterized in part by increased biofilm production[8,10,11]. Consistent with this, the Vc2 riboswitch was found to be an ‘ON’ switch, in that increased c-di-GMP levels result in increased gene expression8. The crystallization construct corresponds to nucleotides 10–98 of the sequence originally reported8. We incorporated a recognition site for the RNA binding domain of the U1A protein into the hairpin loop at the top of the P3 helix to facilitate RNA cocrystallization[12]. The structure was solved using multiwavelength anomalous dispersion (MAD) from a single crystal soaked with iridium hexamine[13].

Riboswitch structure and recognition of c-di-GMP

The c-di-GMP RNA aptamer forms a three-helix y-shaped structure with the ligand binding site at the three-helix junction. The crystal structure reveals that the 5′- and 3′-flanking nucleotides form an additional helix, P1, that includes a canonical G-C base pair with c-di-GMP (Fig. 1). P1 stacks under the P2 helix, and P2 and P3 are parallel to each other. They are aligned via a tetraloop in P2 and a tetraloop receptor in P3 (Fig. 1 and Supplementary Fig. 1). The helical juxtaposition is further stabilized by a phylogenetically conserved, but

structurally isolated, Watson-Crick base pair between C44 in P2 and G83 in P3, both of which are bulged residues in their respective helices (Fig. 1 and Supplementary Fig. 2). The extensive interaction network between P2 and P3 and the lack of modulation as monitored by in-line probing suggest that the P2–P3 segment of the aptamer does not undergo major changes with ligand binding[8].

Although c-di-GMP has a two-fold axis of rotational symmetry, the riboswitch recognizes the second messenger asymmetrically, both in contacts to the bases and to the ribosyl phosphate backbone. One G is recognized by Watson-Crick base-pairing and the other by contacts to the Hoogsteen face. The c-di-GMP binding pocket is composed of residues from P1 and P2 and the joiner regions between the helices, J1/2 and J2/3 (Fig. 1). The top guanosine, G_α, forms a Hoogsteen pair with G20, the first unpaired nucleotide on the 5′ end of P2 (Fig. 2a). The O6 of G_α hydrogen bonds with the exocyclic amine of G20, and the G_α N7 forms a hydrogen bond with N1 of G20. Additional hydrogen bonding contacts are made between the N2 of G_α and the 3′-OH of A48 and the 2′-OH of C46, and between the G_α 2′-OH and a nonbridging phosphate oxygen of A47. Notably, the Watson-Crick surface of G_α is not recognized but instead sits on the edge of a solvent-accessible cavity formed at the junction of the P2 and P3 helices.

The second guanosine of c-di-GMP, G_β, forms a standard Watson-Crick base pair with C92, a highly conserved nucleotide 3′ of P3 (Fig. 2b). The interaction is further supported by hydrogen bonds between the 2′-OH of A47 and the N7 of G_β, between the N1 of A18 and the N2 of G_β, and between the G_β 2′-OH and the exocyclic amine of A18. The G_β-C92 base pair is the first of the P1 helix, the total length of which is 5 base pairs. Inspection of the full-length riboswitch sequence suggests that three additional base pairs could form, but they were not seen here due to the length of the RNA used and the fact that residues on the 5′ end of P1 were involved in crystal packing interactions. Based on the formation of this helix, the aligned c-di-GMP riboswitch sequences were re-examined to reveal that most motifs have the potential to form an imperfect P1 helix (Fig. 1, Supplementary Figs. 3,4, **Supplementary Data** and **Supplementary Methods**). The helix is not conserved in sequence, length or bulged nucleotides, which explains why it was not detected in the initial bioinformatics study.

In addition to hydrogen bonding contacts, the two bases of c-di-GMP participate in an extensive base-stacking network that bridges the P1 and P2 helical stacks. G_α and G_β do not stack directly on each other. Instead A47, a highly conserved base in the J2/3 segment, intercalates between them (Figs. 2c,d). The result is a continuous three-base stack between G_α, A47, and G_β. The stacking interface continues with the G21-C46 base pair above G_α and the G14-C93 base pair below G_β. These interactions likely provide the stabilizing contacts necessary to nucleate formation of the P1 helix.

The phosphate backbone of c-di-GMP is recognized by metal-ion interactions, but like the bases, the two phosphates of the symmetric ligand are recognized asymmetrically (Fig. 2e). The phosphate 5′ of G_α makes an outer-sphere contact to a tightly bound, fully coordinated metal ion. The metal is an iridium hexamine in this structure, but it is likely to be a fully hydrated magnesium ion in the native complex (Data not shown). This phosphate is also contacted by the exocyclic amine of A47. The phosphate 5′ of G_β makes an inner-sphere contact to a magnesium ion though the density for this metal is rather weak. In the MAD electron density (Fig. 2f), two peaks are observed near this phosphate. One peak, ~2σ, is at a distance consistent with it being a magnesium ion (2.4 Å). The other is within hydrogen bonding distance (3.1 Å) and is most likely a water molecule. The weakness of the density may indicate that this metal is not as tightly bound or that the metal is not as localized as the metal contacting the other phosphate.

Measurement of the K_d and rates of ligand binding

We tested predictions resulting from the c-di-GMP riboswitch structure through the use of a gel-shift assay that makes it possible to directly measure the RNA–c-di-GMP interaction using radiolabeled c-di-GMP (Fig. 3a). We used this assay to measure the equilibrium dissociation constant (K_d) for the wild-type RNA construct 110 Vc2, originally measured as approximately 1 nM by in-line probing[8]. This construct is extended on both the 5′ and 3′ ends relative to the RNA used in the crystallographic studies and includes a full-length P1 helix. Unexpectedly, we observed increasing binding with longer incubation times of c-di-GMP with the RNA, which suggests that the complex has a very slow approach to equilibrium. To assess how slow, we measured the on- and off-rates (k_{on} and k_{off}) for ligand binding using a pulse-chase experiment with the gel-shift assay (Figs. 3b,c). The on-rate is 1.0×10^6 M^{-1} min^{-1}, approximately 4 orders of magnitude below the diffusion-controlled limit. This rate is similar to that measured for the adenine binding riboswitch and approximately an order of magnitude slower than that found for the flavin mononucleotide (FMN) binding riboswitch[14,15]. The data fit well to a double exponential, with around 80% reacting at the faster rate. The double-exponential behavior suggests that there may be at least two different starting RNA conformations that bind c-di-GMP at different rates, or that there are multiple steps in the binding reaction. The off-rate is 1.1×10^{-5} min^{-1}, which corresponds to a half-life of approximately 1 month, meaning that ligand binding is effectively irreversible on the biological time scale. This is extremely slow when compared to other riboswitches; 4 and 5 orders of magnitude slower than the FMN and adenine riboswitches, respectively[14,15]. The ratio of k_{off} and k_{on} gives an estimate of the K_d for c-di-GMP binding to the aptamer of approximately 10 pM (Table 1). To our knowledge, this is the tightest affinity measured for an RNA–small molecule interaction.

To verify that measuring the on- and off-rates is an appropriate method of obtaining a K_d in the c-di-GMP riboswitch system, we measured the K_d of the C92U mutant both by the gel-shift assay and by measuring the on- and off-rates (Figs. 3b,d,e). We predicted that this mutation would still allow G_β binding through the formation of a G·U wobble pair with U92 but that the affinity for c-di-GMP would be reduced relative to wild-type. The on-rate of the point mutant was roughly equivalent to that of the wild-type but the off-rate became 1,000-fold faster, with a half-life of approximately 1 hour instead of 1 month. The equilibrium K_d value was obtained by allowing the complex to incubate until no further increase in binding was observed, approximately 22 hours. The K_d values that we obtained from each method were equivalent within experimental error (13 versus 15 nM) (Table 1). These data validate the method and also confirm a structural prediction. Mutation of C92 to a U results in a reduction in binding affinity by more than 3 orders of magnitude. This suggests that there is a substantial energetic cost associated with substituting a G-C pair with a G·U wobble pair at the G_β position.

Selectivity switch of the c-di-GMP riboswitch

To test the overall recognition elements revealed by the structure, we set out to change the selectivity of the c-di-GMP riboswitch aptamer from an RNA responsive to c-di-GMP to one that binds a related molecule, c-di-AMP. Bacteria encode proteins with diadenylate cyclase activity, synthesizing c-di-AMP from ATP[16]. Little is known about the biological function of c-di-AMP, but it is possible that it acts as a second messenger much like c-di-GMP, potentially as a signal for DNA damage[16,17]. The presence of a Watson-Crick base pair in the complex suggested that the C92U mutation would allow similar pairing of A_β to U92. It was not obvious which mutation at G20 would be productive for A_α binding, so all three possible mutations were tested. The wild-type and C92U mutant RNAs have no detectable affinity for c-di-AMP. The G20C/C92U and G20U/C92U double mutants were unable to bind either c-di-GMP or c-di-AMP. However, a selectivity switch was achieved

with the G20A/C92U double mutant. This mutant bound both c-di-GMP and c-di-AMP and showed a four-fold preference for c-di-AMP over c-di-GMP (Fig. 3f and Table 1). A20 could form two hydrogen bonds with A_α if it shifted slightly in its hydrogen bonding register, whereas it could form only one hydrogen bond with G_α. In-line probing of the double mutant with both ligands suggests a binding mode similar to the wild-type RNA with c-di-GMP (Supplementary Fig. 5). This result suggests that naturally occurring c-di-AMP riboswitches may exist, although none of the currently identified c-di-GMP binding sequences have this double mutant combination. If such riboswitches were to be found, they may reveal important information concerning the physiological role of c-di-AMP based on the nature of the genes that lie downstream. Given that this double mutant RNA has affinity for both the adenosine and the guanosine forms of the cyclic dinucleotide, the resulting engineered RNA is the equivalent of an 'OR' switch that can be activated by either of these second messengers.

DISCUSSION

The GEMM riboswitch appears to play a major role in signaling by the second messenger c-di-GMP based on the broad distribution of genes under its control[8]. We found that this riboswitch recognized the ligand c-di-GMP asymmetrically, contacting the Hoogsteen face of G_α and the Watson-Crick face of G_β, and making asymmetric inner-sphere and outer-sphere metal ion contacts with the two phosphates.

The asymmetric recognition of c-di-GMP seen in this riboswitch structure is similar to what has been observed in proteins that also bind this second messenger. The PilZ protein domain has been shown to bind c-di-GMP, and members of this protein family are important in processes regulated by c-di-GMP. Potential modes of action for the PilZ protein family have been suggested, although no specific mechanisms for signaling have emerged[18-23]. The PilZ domain contacts only the Hoogsteen face of G_α and both the Watson-Crick and Hoogsteen faces of G_β, analogous to what is seen in the c-di-GMP riboswitch. The phosphate atoms are also contacted asymmetrically, one with only a single hydrogen bond and the other with multiple contacts[20]. Despite the similarities in contacts to the ligand, the conformations in which proteins bind c-di-GMP differ from that bound by the riboswitch (Supplementary Fig. 6, **Supplementary Discussion**). Stacking interactions with protein side chains also play a role in binding by proteins, but these interactions are not likely to be as favorable as those made with A47, perhaps leading to an alternative conformation of c-di-GMP bound to these proteins[20,24-28]. Overall, the riboswitch provides tight base-pairing and -stacking interactions with other purines. This is reflected in the binding affinity of this RNA, around 10 pM, versus those of the known c-di-GMP binding proteins, which range from low nanomolar to low micromolar[1].

The presence of even a single molecule of c-di-GMP in the cell corresponds to a concentration of approximately 1 nM[1]. If we assume that *in vitro* measurements approximate what occurs in the cell, this is approximately 100-fold above the 10 pM K_d for the riboswitch–c-di-GMP interaction. If the binding affinity alone controlled the 'switch', this RNA would exist exclusively in the bound conformation in the presence of even the slightest amount of c-di-GMP and no biological control would be possible. Regulation therefore is likely to reside in the extremely slow on-rate and off-rate. However, the combination of a slow on-rate and the tight affinity suggests that it would take the complex approximately 100 days (10 half-lives) to reach equilibrium at a concentration equal to the K_d. The off-rate is so slow that the ligand is effectively irreversibly bound in the time frame in which the switch must be triggered. Therefore, this c-di-GMP riboswitch is likely to be kinetically controlled, meaning that the switch is regulated entirely by the on-rate[14,15]. Although the on-rate is also slow, it is a bimolecular rate linearly dependent on the c-di-

GMP concentration, so this c-di-GMP riboswitch is likely to be linearly responsive to ligand across a wide range of concentrations. In the cell, the decision to switch 'ON' or 'OFF' must often be made during transcription of the mRNA, and therefore binding must occur on this time scale, typically on the order of seconds, in order to be biologically relevant. For binding to occur quickly enough, concentrations in the micromolar range may be necessary. This is consistent with the current model in which external signals cause locally and temporally controlled bursts in c-di-GMP concentrations[1].

The structure of the c-di-GMP riboswitch bound to c-di-GMP not only reveals the interactions important for ligand binding and recognition in this system, but also presents a detailed view of c-di-GMP interacting with a downstream target, providing insight into how this second messenger regulates gene expression on the molecular level. It reveals that formation of the P1 helix, which had not previously been identified in the secondary structure of this riboswitch, accompanies ligand binding. P1 is formed from the 5′ and 3′ ends of the RNA. These ends appear to be less structured in the ligand-free form of the riboswitch based on in-line probing[8]. This information combined with the crystal structure leads to the hypothesis that when c-di-GMP binds to the aptamer, it locks the 3′ end of the RNA into a specific conformation through base pairing with C92, initiating the formation of the P1 helix. It appears that P1 helix formation in the c-di-GMP riboswitch class is the molecular trigger that adjusts gene expression levels in response to c-di-GMP levels. The formation or disruption of P1 helices formed from the 5′ and 3′ ends of riboswitch aptamers is predicted to be an essential component of the expression platform of many other riboswitch classes, independent of whether the riboswitch functions in transcriptional or translational regulation[29-32]. c-di-GMP riboswitches are predicted to use both types of control[8] and inspection of these riboswitch sequences reveals potential expression platforms involving the P1 stem (see Supplementary Fig. 7). This RNA element therefore allows c-di-GMP signaling to directly control the expression of a diverse group of genes in response to c-di-GMP binding.

Supplementary Material

Refer to Web version on PubMed Central for supplementary material.

Acknowledgments

We thank S. Myers and the beamline staff at X25, X12C and X29 at the National Synchrotron Light Source at Brookhaven National Laboratory; M. Strickler, D. Keller, and the Yale Center for Structural Biology core staff; Y. Xiong for data processing help and advice; C. Shanahan, E. Butler, N. Carrasco, J. Cochrane and M. Stahley for help and advice; D. Hiller, J. Davis, E. Lee, N. Sudarsan and other members of the Strobel and Breaker labs for helpful discussions; V. Singh (Strobel lab) for synthesis of iridium hexamine; U. Jenal (U. of Basel) for the gift of the PleD* expression plasmid; K.-P. Hopfner (U. of Munich) for the gift of the DisA expression plasmid; and G. Reguera (Michigan State U.) and B. Bassler (Princeton U.) for the gift of *V. cholerae* genomic DNA. This work was supported by the US National Institutes of Health grant GM02278 to S.A.S.

ONLINE METHODS

RNA crystallization and structure determination

We cloned riboswitch sequences from genomic DNA and transcribed and purified them as previously described[34]. c-di-GMP was chemically synthesized following previously published procedures with minor modifications[35]. The primary differences were modifications to the final deprotections where *N*-methylamine and aqueous ammonia were used in place of only aqueous ammonia. The U1A protein (Y31H, Q36R double mutant) was expressed and purified as previously described[12]. A solution containing 100 μM riboswitch RNA and 215 μM c-di-GMP was heated to 70 °C and slow cooled in folding

buffer containing 10 mM $MgCl_2$, 10 mM KCl, and 10 mM sodium cacodylate, pH 6.8. The cocrystallization protein U1A was added at a final concentration of 140 μM and the complex was allowed to equilibrate for 1 h. This solution was then mixed in a 1:1 ratio with well solution: 22% (v/v) polyethylene glycol monomethyl ether 550 (PEG MME 550), 5 mM $MgSO_4$, 50 mM MES, pH 6.0, and 0.3 M NaCl. Crystals were grown at 25 °C using hanging-drop vapor diffusion. Crystals appeared within 2 d and grew in large clusters that could be broken apart to produce single crystals with a maximum size of 400 μm × 50 μm × 5 μm. Crystals were stabilized in mother liquor with 30% (v/v) PEG MME 550 and flash frozen in liquid nitrogen. For phasing, crystals were soaked in stabilization solution with the addition of 1 mM iridium hexamine for approximately 3 h before flash freezing. Three-wavelength MAD data were collected at 100 K at beamline X29 at NSLS (Table 2). Iridium hexamine was synthesized as described previously13. Data were processed using HKL2000 (ref. 36). Initial phase information was obtained by locating the U1A protein by molecular replacement using Phaser37. Initial heavy atom sites were located by difference Fourier methods and used in Solve to generate initial maps38. Nine iridium sites were located and the solution had a *Z* score of 46.2 and a figure of merit of 0.43. Solvent flattening was performed using Resolve[39]. Model building was done in Coot[40], and Refmac[41] and CNS[42,43] were used for refinement (Table 2). Figures were made in PyMol (DeLano Scientific)[44].

K_d and rate measurements of wild-type and mutant RNAs

Riboswitch RNAs containing point mutations were cloned using site-directed mutagenesis. Radiolabeled c-di-GMP was obtained enzymatically according to published procedures and purified by polyacrylamide gel electrophoresis (PAGE)[45,46]. A constitutively active diguanylate cyclase, PleD*, was expressed and purified as described, and the reaction was initiated using [α-^{32}P]GTP as the substrate[45]. As the reaction proceeded, a single band appeared that ran more slowly than the starting material on the PAGE purification gel. Radiolabeled c-di-AMP was obtained similarly, using the protein DisA and [α-^{32}P]ATP as the substrate[16]. 110 Vc2 riboswitch RNAs were folded in the presence of radiolabeled ligand and folding buffer. The complex was allowed to equilibrate for 1 hour or greater at room temperature, and bound and free c-di-GMP were separated by native (100 mM Tris/HEPES pH 7.5, 10 mM $MgCl_2$, 0.1 mM EDTA) PAGE at 4 °C. A STORM PhosphoImager (GE Healthcare) was used to scan gels, and the bands were quantified using ImageQuant (GE Healthcare). Fraction bound was graphed versus RNA concentration and fit using KaleidaGraph (Synergy Software) to obtain K_ds according to the equation:

$$F = (F_\infty * C) / (C + K_d)$$

where F = fraction bound, F_∞ = fraction bound at saturation and C = riboswitch concentration.

To measure the off-rate of ligand binding, RNA and a trace amount of radiolabeled c-di-GMP in the presence of folding buffer were allowed to come to equilibrium. A competition reaction was then initiated by adding a 100-fold excess of unlabeled c-di-GMP, and the mixture was incubated for various periods of time before loading the reaction on a native polyacrylamide gel. Because the off-rate is so slow for the wild-type 110 Vc2 sequence, only the linear portion of the curve could be measured, and the fractional dissociation of the labeled c-di-GMP as a function of time provided an estimate of the off-rate according to:

$$F = -kt + F_0$$

where k = rate, t = time and F_0 = fraction bound at time $t = 0$. For the C92U mutant, the off-rate was obtained from the following equation:

$$F=F_{\infty}+Ae^{-kt}$$

where F_{∞}=fraction bound at time=∞ and A = amplitude.

Because the 110 Vc2 off-rate measurement required such a long incubation time (more than 1 month), a sample of RNA with no c-di-GMP was used as a control for RNA degradation. It was placed at room temperature for the entire length of the experiment and radiolabeled c-di-GMP was added at the end. A complete gel shift was observed, indicating that a sufficient fraction of the RNA remained for complete ligand binding. If RNA degradation did occur, the measurements reported would overestimate the true off-rate, resulting in an even tighter K_d.

The on-rate was measured using a similar approach. The excess unlabeled c-di-GMP was added a variable period of time after the RNA and labeled c-di-GMP were mixed together, and the reaction was immediately loaded onto the gel. We found that the data for the 110 Vc2 sequence did not fit well to a single-exponential equation, so we fit the data using a double-exponential expression where 80% reacts at the faster rate k_1:

$$F=A_1\left(1-e^{-k_1t}\right)+A_2\left(1-e^{-k_2t}\right)$$

k_1 was used to calculate the on-rate. The data for the C92U mutant fit well to a single-exponential equation:

$$F=A\left(1-e^{-kt}\right)$$

In the case of the single exponential, the amplitude term represents the total fraction bound at equilibrium. In the double-exponential fit, it is not possible to completely define the amplitude term without additional information about the mechanism of the binding reaction (see Discussion).

References

1. Hengge R. Principles of c-di-GMP signalling in bacteria. Nat. Rev. Microbiol 2009;7:263–273. [PubMed: 19287449]
2. Römling U, Amikam D. Cyclic di-GMP as a second messenger. Curr. Opin. Microbiol 2006;9:218–228. [PubMed: 16530465]
3. Tamayo R, Pratt JT, Camilli A. Roles of cyclic diguanylate in the regulation of bacterial pathogenesis. Annu. Rev. Microbiol 2007;61:131–148. [PubMed: 17480182]
4. Waters CM, Lu W, Rabinowitz JD, Bassler B. Quorum sensing controls biofilm formation in *Vibrio cholerae* through modulation of cyclic di-GMP levels and repression of vpsT. J. Bacteriol 2008;190:2527–2536. [PubMed: 18223081]
5. Fong JC, Yildiz F. Interplay between cyclic AMP-cyclic AMP receptor protein and cyclic di-GMP signaling in *Vibrio cholerae* biofilm formation. J. Bacteriol 2008;190:6646–6659. [PubMed: 18708497]
6. Jenal U, Malone J. Mechanisms of cyclic-di-GMP signaling in bacteria. Annu. Rev. Genet 2006;40:385–407. [PubMed: 16895465]

7. Ryan R, Fouhy Y, Lucey J, Dow JM. Cyclic di-GMP signaling in bacteria: recent advances and new puzzles. J. Bacteriol 2006;188:8327–8334. [PubMed: 17028282]
8. Sudarsan N, et al. Riboswitches in eubacteria sense the second messenger cyclic di-GMP. Science 2008;321:411–413. [PubMed: 18635805]
9. Roth A, Breaker RR. The structural and functional diversity of metabolite-binding riboswitches. Annu. Rev. Biochem 2009;78:305–334. [PubMed: 19298181]
10. Lim B, Beyhan S, Meir J, Yildiz F. Cyclic-diGMP signal transduction systems in *Vibrio cholerae*: modulation of rugosity and biofilm formation. Mol. Microbiol 2006;60:331–348. [PubMed: 16573684]
11. Beyhan S, Yildiz F. Smooth to rugose phase variation in *Vibrio cholerae* can be mediated by a single nucleotide change that targets c-di-GMP signalling pathway. Mol. Microbiol 2007;63:995–1007. [PubMed: 17233827]
12. Ferré-D'Amaré AR, Doudna JA. Crystallization and structure determination of a hepatitis delta virus ribozyme: use of the RNA-binding protein U1A as a crystallization module. J. Mol. Biol 2000;295:541–556. [PubMed: 10623545]
13. Galsbol FH, Simonsen K. The preparation, separation and characterization of some ammine complexes of Iridium(III). Acta Chem. Scand 1990;44:796–801.
14. Wickiser JK, Cheah M, Breaker R, Crothers DM. The kinetics of ligand binding by an adenine-sensing riboswitch. Biochemistry 2005;44:13404–13414. [PubMed: 16201765]
15. Wickiser JK, Winkler W, Breaker R, Crothers DM. The speed of RNA transcription and metabolite binding kinetics operate an FMN riboswitch. Mol. Cell 2005;18:49–60. [PubMed: 15808508]
16. Witte G, Hartung S, Büttner K, Hopfner KP. Structural biochemistry of a bacterial checkpoint protein reveals diadenylate cyclase activity regulated by DNA recombination intermediates. Mol. Cell 2008;30:167–178. [PubMed: 18439896]
17. Römling U. Great times for small molecules: c-di-AMP, a second messenger candidate in Bacteria and Archaea. Sci. Signal 2008;1:pe39. [PubMed: 18714086]
18. Amikam D, Galperin M. PilZ domain is part of the bacterial c-di-GMP binding protein. Bioinformatics 2006;22:3–6. [PubMed: 16249258]
19. Ryjenkov DA, Simm R, Römling U, Gomelsky M. The PilZ domain is a receptor for the second messenger c-di-GMP: the PilZ domain protein YcgR controls motility in enterobacteria. J. Biol. Chem 2006;281:30310–30314. [PubMed: 16920715]
20. Benach J, et al. The structural basis of cyclic diguanylate signal transduction by PilZ domains. EMBO J 2007;26:5153–5166. [PubMed: 18034161]
21. Christen M, et al. DgrA is a member of a new family of cyclic diguanosine monophosphate receptors and controls flagellar motor function in *Caulobacter crescentus*. Proc. Natl. Acad. Sci. USA 2007;104:4112–4117. [PubMed: 17360486]
22. Merighi M, Lee V, Hyodo M, Hayakawa Y, Lory S. The second messenger bis-(3′-5′)-cyclic-GMP and its PilZ domain-containing receptor Alg44 are required for alginate biosynthesis in Pseudomonas aeruginosa. Mol. Microbiol 2007;65:876–895. [PubMed: 17645452]
23. Pratt JT, Tamayo R, Tischler A, Camilli A. PilZ domain proteins bind cyclic diguanylate and regulate diverse processes in Vibrio cholerae. J. Biol. Chem 2007;282:12860–12870. [PubMed: 17307739]
24. Minasov G, et al. Crystal structures of YkuI and its complex with second messenger c-di-GMP suggests catalytic mechanism of phosphodiester bond cleavage by EAL domains. J. Biol. Chem 2009;284:13174–13184. [PubMed: 19244251]
25. Barends TRM, et al. Structure and mechanism of a bacterial light-regulated cyclic nucleotide phosphodiesterase. Nature 2009;459:1015–1018. [PubMed: 19536266]
26. Chan C, et al. Structural basis of activity and allosteric control of diguanylate cyclase. Proc. Natl. Acad. Sci. USA 2004;101:17084–17089. [PubMed: 15569936]
27. Wassmann P, et al. Structure of BeF3--modified response regulator PleD: implications for diguanylate cyclase activation, catalysis, and feedback inhibition. Structure 2007;15:915–927. [PubMed: 17697997]
28. De N, et al. Phosphorylation-independent regulation of the diguanylate cyclase WspR. PLoS Biol 2008;6:e67. [PubMed: 18366254]

29. Winkler W, Cohen-Chalamish S, Breaker R. An mRNA structure that controls gene expression by binding FMN. Proc. Natl. Acad. Sci. USA 2002;99:15908–15913. [PubMed: 12456892]
30. Mandal M, Boese B, Barrick J, Winkler W, Breaker R. Riboswitches control fundamental biochemical pathways in *Bacillus subtilis* and other bacteria. Cell 2003;113:577–586. [PubMed: 12787499]
31. Winkler W, Nahvi A, Sudarsan N, Barrick J, Breaker R. An mRNA structure that controls gene expression by binding *S*-adenosylmethionine. Nat. Struct. Biol 2003;10:701–707. [PubMed: 12910260]
32. Sudarsan N, et al. An mRNA structure in bacteria that controls gene expression by binding lysine. Gend. Dev 2003;17:2688–2697.
33. Leontis NB, Westhof E. Geometric nomenclature and classification of RNA base pairs. RNA 2001;7:499–512. [PubMed: 11345429]
34. Cochrane JC, Lipchock SV, Strobel S. Structural investigation of the GlmS ribozyme bound to Its catalytic cofactor. Chem. Biol 2007;14:97–105. [PubMed: 17196404]
35. Hyodo M, Hayakawa Y. An Improved Method for Synthesizing Cyclic Bis(3′–5′)diguanylic Acid (c-di-GMP). Bull. Chem. Soc. Jpn 2004;77:2089–2093.
36. Otwinowski Z, Minor W. Processing of X-ray diffraction data collected in oscillation mode. Methods Enzymol 1997;276:307–326.
37. McCoy AJ, Grosse-Kunstleve RW, Storoni LC, Read RJ. Likelihood-enhanced fast translation functions. Acta Crystallogr. D Biol. Crystallogr 2005;61:458–464. [PubMed: 15805601]
38. Terwilliger TC, Berendzen J. Automated MAD and MIR structure solution. Acta Crystallogr. D Biol. Crystallogr 1999;55:849–861. [PubMed: 10089316]
39. Terwilliger TC. Maximum-likelihood density modification. Acta Crystallogr. D Biol. Crystallogr 2000;56:965–972. [PubMed: 10944333]
40. Emsley P, Cowtan K. Coot: model-building tools for molecular graphics. Acta Crystallogr. D Biol. Crystallogr 2004;60:2126–2132. [PubMed: 15572765]
41. Winn MD, Isupov MN, Murshudov GN. Use of TLS parameters to model anisotropic displacements in macromolecular refinement. Acta Crystallogr. D Biol. Crystallogr 2001;57:122–133. [PubMed: 11134934]
42. Brunger AT, et al. Crystallography & NMR System (CNS), a new software suite for macromolecular structure determination. Acta Crystallogr. D Biol. Crystallogr 1998;54:905–921. [PubMed: 9757107]
43. Brunger AT. Version 1.2 of the Crystallography and NMR System. Nat. Protocols 2007;2:2728–2733.
44. DeLano, WL. The Pymol Molecular Graphics System. 2008.
45. Paul R, et al. Cell cycle-dependent dynamic localization of a bacterial response regulator with a novel di-guanylate cyclase output domain. Gend. Dev 2004;18:715–727.
46. Christen M, Christen B, Folcher M, Schauerte A, Jenal U. Identification and characterization of a cyclic di-GMP-specific phosphodiesterase and its allosteric control by GTP. J. Biol. Chem 2005;280:30829–30837. [PubMed: 15994307]

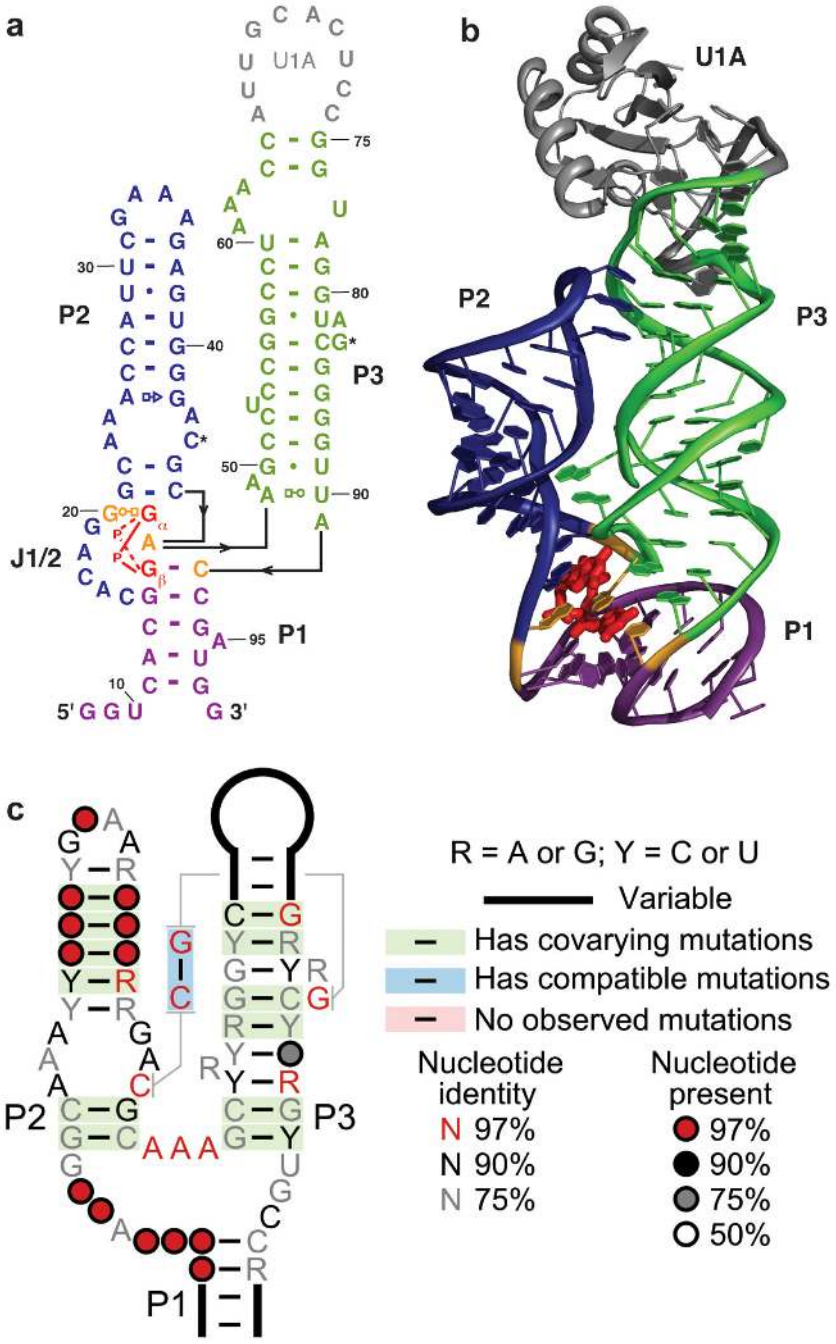

Figure 1.

Structure of the c-di-GMP riboswitch aptamer. (**a**) Secondary structure representation of the crystallized c-di-GMP aptamer. Helices P1, P2, and P3 are colored purple, blue, and green respectively. c-di-GMP is shown in red. Nucleotides that directly contact c-di-GMP are shown in orange. The U1A cocrystallization protein is shown in gray. Numbering is the same as previously published for this sequence[8]. Watson-Crick base pairs are denoted by dashes, all other base pairs are indicated using the nomenclature of Westhof and Leontis[33]. A * indicates a Watson-Crick base pair in the tertiary structure. The two guanines of c-di-GMP are denoted G_α and G_β for clarity. (**b**) Representation of the crystal structure of the Vc2 c-di-GMP riboswitch aptamer from *V. cholerae*. Coloring is the same as used in **a**. (**c**)

Revised consensus sequence and secondary structure model of the c-di-GMP aptamer (see **Supplementary Fig.** 3). Nucleotides are colored to reflect their percent conservation. The structurally isolated Watson-Crick base pair is shown with gray lines connecting the nucleotide in P2 with the other in P3.

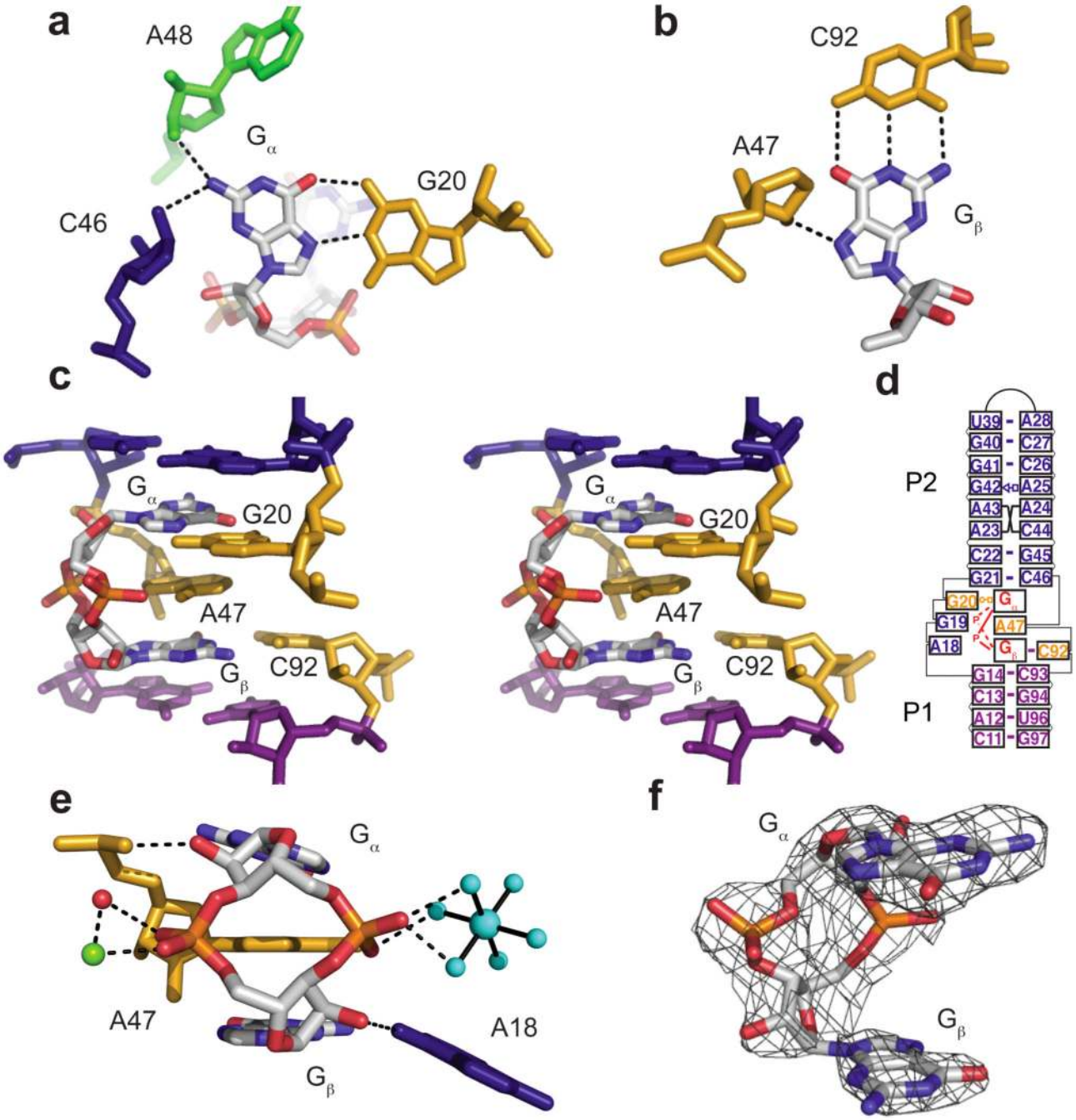

Figure 2.

Recognition of c-di-GMP by the riboswitch. Coloring of nucleotides is the same as in Figure 1. Hydrogen bonds are denoted by dashed lines. (**a**) The Hoogsteen face of G_α is recognized by G20 and the N2 of G_α is contacted by C46 and A48. (**b**) G_β forms a canonical Watson-Crick base pair with C92. The N7 of G_β is contacted by A47. (**c**) Stereo view of the extensive stacking interactions made in the binding pocket. A conserved adenosine, A47, stacks directly between G_α and G_β. (**d**) Stacking interactions in the binding pocket bridge the P1 and P2 helices. (**e**) Recognition of the ribosyl phosphate backbone is primarily through hydrogen bonding to the RNA as well as metal mediated contacts. Iridium hexamine is

shown in cyan, magnesium in green, and water in red. (**f**) MAD electron density observed for c-di-GMP contoured at 1σ.

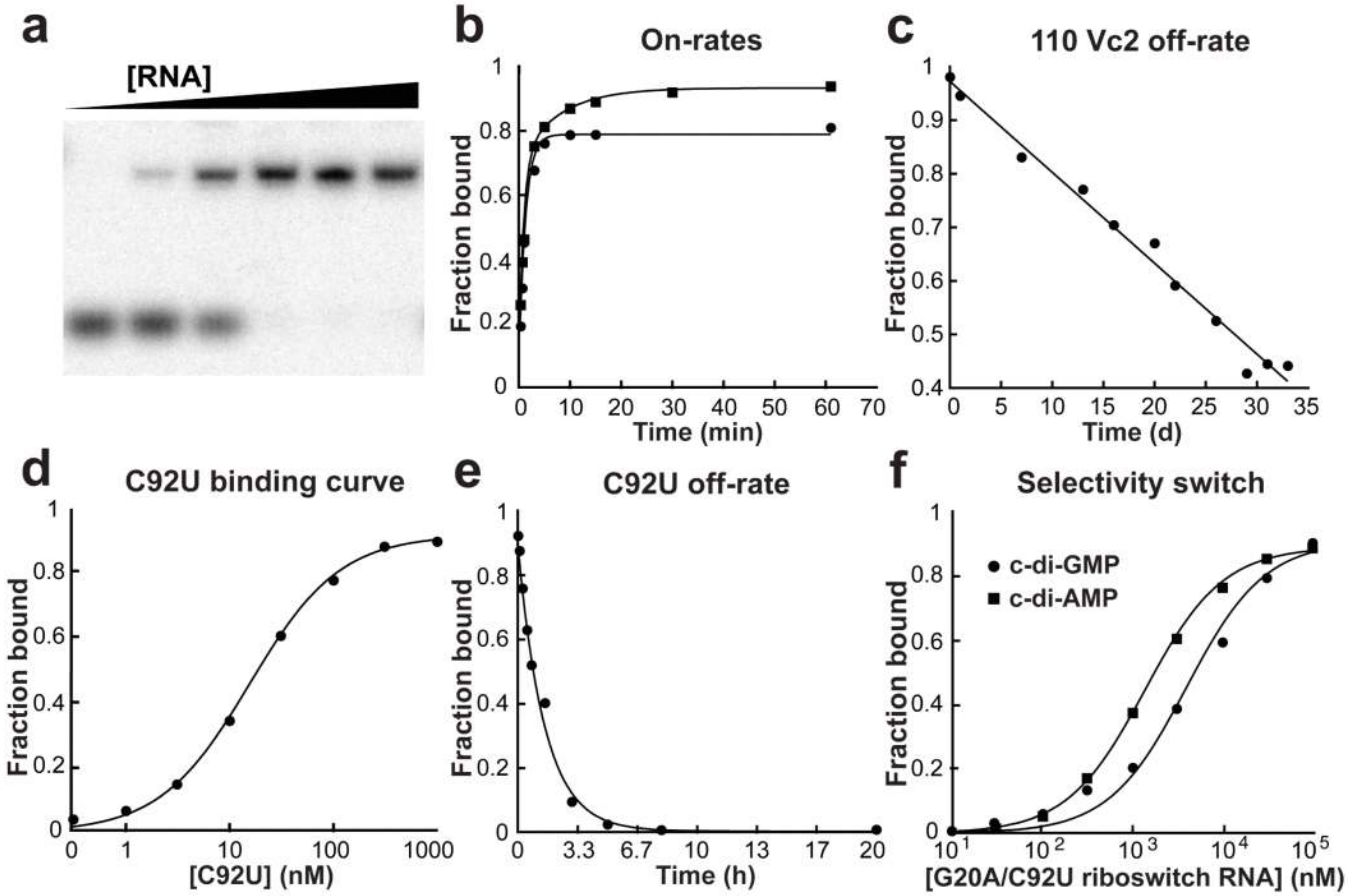

Figure 3.

Affinity and rate measurements for c-di-GMP binding to wild-type and mutant riboswitches. (**a**) Gel-shift assay. Radiolabeled c-di-GMP is incubated with riboswitch RNA and then bound (top band) and free c-di-GMP (bottom band) are separated using polyacrylamide gel electrophoresis (PAGE). (**b**) On-rate curves of c-di-GMP binding to the 110 Vc2 wild-type RNA (squares) and C92U mutant RNA binding to c-di-GMP (circles). k_{on} was obtained by dividing the observed rate (k_{obs}) by the concentration of RNA used in the experiment (1 μM). (**c**) Off-rate for the dissociation of the 110 Vc2 wild-type RNA–c-di-GMP complex. Because the off-rate is so slow, only the linear region of the curve could be measured and the off-rate was estimated from the slope. (**d**) Binding curve for C92U mutant RNA binding to c-di-GMP. (**e**) Off-rate for the dissociation of the C92U mutant RNA–c-di-GMP complex. (**f**) Binding curves for the G20A/C92U double mutant RNA binding to c-di-GMP (circles) and c-di-AMP (squares).

Table 1

Binding rates and affinities for wild-type and mutant c-di-GMP riboswitches

[AU: Please check table titles and captions are complete, as we were unable to edit some material directly (th is appeared in so-called Word "text boxes").]

RNA	Off-rate (min^{-1})	$t_{1/2}$[a] (min)	On-rate (M^{-1} min^{-1})	c-di-GMP, calculated[c]	K_d Values (nM) c-di-GMP, measured	c-di-AMP, measured
110 Vc2	$1.1 \pm 0.082 \times 10^{-5}$	6.3×10^4	1.0[b] $\pm 0.016 \times 10^6$	0.011	–[d]	n.d.[e]
C92U	$1.0 \pm 0.16 \times 10^{-2}$	69	$8.0 \pm 0.99 \times 10^5$	13	15 ± 1.1	n.d.
G20A, C92U	–	–	–	–	4,900 ± 960	1,200 ± 130
G20C, C92U	–	–	–	–	n.d.[f]	n.d.
G20U, C92U	–	–	–	–	n.d.	n.d.

[a] $t_{1/2}$ is the half-life of the complex and was calculated from the dissociation rate.

[b] The on-rate data for 110 Vc2 was biphasic. This rate was calculated from the rate corresponding to 80% of the amplitude.

[c] The calculated K_d results from taking the ratio of the off-rate and the on-rate of ligand binding.

[d] A dash means that the measurement was not attempted.

[e] n.d. means no binding was detected up to 100 μM ligand.

[f] A small smear was observed at 100 μM RNA indicating some binding, but the K_d is not measurable with this assay. Reported values are the average of at least three trials ± s.d.

Table 2
Data collection and refinement statistics

	1 mM iridium hexamine soak		
Data collection			
Space group		$P2_1$	
Cell dimensions			
a, b, c (Å)		49.5, 45.1, 76.6	
α, β, γ (°)		90.0, 96.8, 90.0	
	Peak	*Inflection*	*Remote*
Wavelength (Å)	1.105	1.1054	1.0762
Resolution (Å)	50–2.7 (2.80–2.70)[a]	50–2.7 (2.80–2.70)	50–2.7 (2.80–2.70)
R_{merge}	0.072 (0.382)	0.072 (0.428)	0.069 (0.448)
$I/\sigma I$	12.5 (1.9)	12.7 (1.7)	13.0 (1.7)
Completeness (%)	97.4 (82.4)	96.3 (77.0)	98.0 (86.9)
Redundancy	2.7 (2.0)	2.7 (1.9)	2.7 (2.1)
Refinement			
Resolution (Å)		50–2.7 (2.77–2.70)	
No. reflections		9,672 (477)	
R_{work}/R_{free}		19.3/25.3 (31.5/47.4)	
No. atoms			
Protein		734	
RNA		1,961	
c-di-GMP		46	
Ions		65	
Water		87	
B-factors			
Protein		54.3	
RNA		47.1	
c-di-GMP		26.9	
Ions		71.8	
Water		47.5	
R.m.s. deviations			
Bond lengths (Å)		0.0058	
Bond angles (°)		1.078	

[a]Highest-resolution shell is shown in parentheses.